Coupled Nd and B' spin ordering in the double perovskites $Nd_2NaB'O_6$ (B' = Ru, Os)

A. A. Aczel,[1,*] D. E. Bugaris,[2] J. Yeon,[2] C. de la Cruz,[1] H.-C. zur Loye,[2] and S. E. Nagler[1,3]

[1]*Quantum Condensed Matter Division, Neutron Sciences Directorate, Oak Ridge National Laboratory, Oak Ridge, Tennessee 37831, USA*

[2]*Department of Chemistry and Biochemistry, University of South Carolina, Columbia, South Carolina 29208, USA*

[3]*CIRE, University of Tennessee, Knoxville, Tennessee 37996, USA*

(Received 24 April 2013; published 15 July 2013)

We present a neutron powder-diffraction study of the monoclinic double perovskite systems $Nd_2NaB'O_6$ (B' = Ru, Os), with magnetic atoms occupying both the A and B' sites of the $A_2BB'O_6$ structure. Our measurements reveal coupled spin ordering between the Nd and B' atoms with magnetic transition temperatures of 14.3(1) K for Nd_2NaRuO_6 and 16.2(2) K for Nd_2NaOsO_6. There is a type-I antiferromagnetic structure associated with the Ru and Os sublattices, with the ferromagnetic planes stacked along the c axis and [110] direction respectively, while the Nd sublattices exhibit complex, canted antiferromagnetism with different spin arrangements in each system.

DOI: 10.1103/PhysRevB.88.014413 PACS number(s): 75.40.Cx, 75.47.Lx, 76.30.He

Double perovskites with the formula $A_2BB'O_6$ have attracted considerable interest recently from both applied and fundamental physics perspectives. The excitement from the applied physics community has largely centered around the observation of room-temperature colossal magnetoresistance coupled with half metallic behavior in Sr_2FeMoO_6.[1] These unique properties ensure a high degree of spin polarization of the charge carriers in a useful temperature regime applicable to potential spintronics devices.[2]

On the fundamental side, double perovskite systems provide excellent opportunities to study geometric frustration on the B'-site face-centered-cubic (fcc) sublattice while tuning both the spin quantum number S and spin-orbit coupling. Past efforts have found several exotic magnetic ground states, mostly in systems characterized by quantum spins of $S = 1/2$ or 1. The diverse magnetism includes a collective singlet state coexisting with paramagnetism in Ba_2YMoO_6,[3,4] a collective singlet state in La_2LiReO_6,[5] spin freezing without long-range order in Ba_2YReO_6,[5] Sr_2MgReO_6,[6] and Sr_2CaReO_6,[7] short-range order in La_2LiMoO_6,[3] and a ferromagnetic (FM) Mott insulating state in Ba_2NaOsO_6.[8,9] Theoretical studies have also indicated that a wealth of other magnetic ground states are possible in these 4d and 5d double perovskite quantum spin systems.[10,11]

Some of the most interesting physical and magnetic properties observed in the double perovskite family can be attributed to the interactions between different types of magnetic atoms on the B and B' sites. For example, the colossal magnetoresistance and half metallic behavior of Sr_2FeMoO_6 and related systems[12] arises from an antiferromagnetic coupling between the delocalized 4d or 5d electrons and the localized 3d electrons. Moreover, the systems Bi_2FeCrO_6 (Refs. 13–15) and Bi_2NiMnO_6 (Ref. 16) are rare examples of multiferroics with both large spontaneous magnetization and polarization. Bi_2NiMnO_6 exhibits ferromagnetic properties, resulting from distributing two types of transition-metal ions with and without e_g electrons in a rocksalt configuration,[17] while Bi_2FeCrO_6 is a ferrimagnet.

In contrast to the extensive studies performed on the subset of double perovskites with magnetic B and B' sites, systems with magnetic ions on both the A and B' sites remain largely unexplored territory. Exploratory synthesis via solid-state reactions and hydroxide flux methods[18] have produced a series of these materials, including R_2NaRuO_6,[19] R_2NaOsO_6,[20] R_2LiOsO_6,[21] and R_2MgIrO_6[22] (R = rare earth), but the magnetic properties have generally only been investigated with bulk probes such as magnetic susceptibility. One exception is the recent work of Ref. 23, where neutron diffraction was used to investigate magnetic ordering in the systems R_2LiRuO_6 (R = Nd, Tb, Pr). The authors found that all three compositions showed evidence for long-range magnetic order, with the Ru sublattice exhibiting common type-I antiferromagnetic (AF) order and the spins of the rare-earth atoms forming a canted arrangement. It is also interesting to note that the magnetic transitions involved coupled spin ordering of the two magnetic sublattices with T_c's > 10 K, while in several double perovskite systems with only an A-site rare-earth magnetic sublattice, no magnetic ordering has been observed in susceptibility measurements down to 2 K.[24,25] These observations indicate that the magnetic behavior of the rare-earth ions in these systems is very sensitive to the presence of other types of magnetic atoms.

The syntheses, crystal structures (shown in Fig. 1), and magnetic susceptibilities of the monoclinic double perovskites Nd_2NaRuO_6 and Nd_2NaOsO_6 were recently reported.[19,20] These materials combine a small A site cation with a relatively large ionic radii difference between the B and B' sites, and therefore exhibit very large, room-temperature structural distortions relative to most other double perovskites. Comparing the Nd_2NaRuO_6 and Nd_2NaOsO_6 magnetization and magnetic susceptibility results to La_2NaRuO_6 and La_2NaOsO_6 clearly shows that the addition of the magnetic rare-earth sublattice dramatically alters the magnetic properties of these materials. For example, the Curie-Weiss temperatures for La_2NaRuO_6 and La_2NaOsO_6 are -57 K and -74 K,[26] while the values for Nd_2NaRuO_6 and Nd_2NaOsO_6 are much closer to 0 and found to be -7 K (Ref. 19) and 3 K.[20] Also, the small deviation from the Curie-Weiss law with decreasing temperature in the susceptibility of La_2NaRuO_6 is replaced by a large ferromagneticlike increase in the susceptibility for Nd_2NaRuO_6, and significant magnetic hysteresis is observed

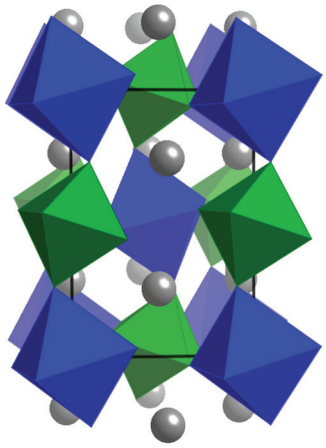

FIG. 1. (Color online) Double perovskite structure, with the large blue octahedra representing NaO_6, the small green octahedra depicting $B'O_6$, and the isolated gray spheres corresponding to Nd atoms. The small ionic radius of Nd leads to a large tilting of the NaO_6 and $B'O_6$ octahedra in Nd_2NaRuO_6 and Nd_2NaOsO_6.

in the M vs H curve for the Nd system that is absent in the La case. Finally, a ferromagneticlike increase with decreasing temperature in the susceptibility of La_2NaOsO_6 gives way to complicated magnetic behavior for Nd_2NaOsO_6, likely indicative of a spin-flop transition for an applied field of 1.7 T at $T = 2$ K.

In this work, neutron powder-diffraction (NPD) measurements have been performed on the double perovskites Nd_2NaRuO_6 and Nd_2NaOsO_6. These specific materials were chosen in an effort to better understand how the unconventional magnetism in La_2NaRuO_6 and La_2NaOsO_6 (Ref. 26) evolves when an exchange path between the A and B' sites is added to these materials. To produce a large enough yield of both materials for the diffraction experiments, solid-state synthesis methods were required. For polycrystalline Nd_2NaRuO_6, Nd_2O_3 (Alfa Aesar, 99.99%) was first activated by heating in air at 1000 °C for 12 h, Na_2CO_3 (Mallinckrodt, 99.95%) was dried overnight at 150 °C, and RuO_2 was prepared by heating Ru (Engelhard, 99.95%) in air at 1000 °C for 24 h. The starting materials were then mixed together in a 1:0.55:1 ratio, and this included a 10% molar excess of Na_2CO_3 to offset the volatilization of Na_2O during heating. This mixture was heated to 500 °C in 1 h, held at 500 °C for 8 h, heated to 900 °C in 1 h, and held at 900 °C for 12 h before turning off the furnace and allowing the sample to cool to room temperature. Powder x-ray diffraction showed the presence of Nd_2NaRuO_6, as well as Nd_2O_3 and Nd_3RuO_7 impurities. Therefore, the sample was ground together with additional Na_2CO_3 and RuO_2, and then subjected to the same heating profile. Due to remaining impurities as confirmed by powder x-ray diffraction, this process was repeated twice more. Finally, all the peaks in the powder pattern could be indexed in the monoclinic space group $P2_1/n$ with lattice parameters in good agreement with those reported for Nd_2NaRuO_6.[19]

For polycrystalline Nd_2NaOsO_6, the starting materials were nearly identical, with the only difference being that Os (J&J Materials Inc.) replaced RuO_2. The heat treatment was also slightly modified, as the starting mixture was heated to 700 °C in 1 h and held at 700 °C for 6 h, before turning off the furnace and allowing the sample to cool to room temperature. Powder x-ray diffraction showed the presence of Nd_2NaOsO_6, as well as Nd_2O_3 and Nd_3OsO_7 impurities. Therefore, the sample was ground together with additional Na_2CO_3 and Os, and then subjected to the same heating profile. Due to remaining impurities as confirmed by powder x-ray diffraction, this process was repeated four more times. Finally, all the peaks in the powder pattern could be indexed in the monoclinic space group $P2_1/n$ with lattice parameters in good agreement with those reported for Nd_2NaOsO_6.[20]

For the neutron powder-diffraction experiments, roughly 5 g of each polycrystalline sample was loaded in a closed-cycle refrigerator and studied using the HB-2A powder diffractometer and HB-1A triple axis spectrometer at the High Flux Isotope Reactor of Oak Ridge National Laboratory. Data from HB-2A were collected with neutron wavelengths $\lambda = 1.54$ Å and $\lambda = 2.41$ Å at temperatures of 4–50 K using a collimation of 12′ before the monochromator, no collimation between the monochromator and sample, and a collimation of 6′ between the sample and detectors. The shorter wavelength gives a greater intensity and higher Q coverage that was used to investigate the crystal structures in this low temperature regime, while the longer wavelength gives lower Q coverage and greater resolution that was important for investigating the magnetic structures of these materials. The NPD data were analyzed using the Rietveld refinement program FULLPROF[27] and the representational analysis software SARAH.[28] HB-1A was used to measure careful order parameter curves of each material, with collimations of 40′ before the monochromator, 40′ between the monochromator and sample, 40′ between the sample and analyzer, and 80′ between the analyzer and detector.

Our neutron-diffraction results for Nd_2NaRuO_6 and Nd_2NaOsO_6 reveal that the Nd and B' spins order at the same temperature with very similar magnetic structures to the Nd_2LiRuO_6 analog.[23] More specifically, the B' sublattices are characterized by type-I antiferromagnetic order with the ferromagnetic planes stacked along the c axis and the [110] direction in the Ru and Os compositions respectively, while the Nd sublattices form different canted arrangements in the two materials. The extra Nd-O-B' exchange interactions in these materials have a significant effect on the magnetism, effectively destroying the delicate balance of extended superexchange interactions that lead to the incommensurate magnetic structure of La_2NaRuO_6 and the drastically reduced ordered moment of La_2NaOsO_6.

Figure 2 shows $\lambda = 1.54$ Å NPD data at $T = 50$ K for monoclinic Nd_2NaRuO_6 and Nd_2NaOsO_6, while Table I shows the refinement parameters extracted from the $T = 4$ K data. Comparing these results with previous x-ray-diffraction data collected on single crystals at room temperature[19,20] reveals no evidence for a structural phase transition between 300 and 4 K in either material, and the structural distortion remains large at all temperatures as indicated by the 4-K β values of 90.898(3)° and 90.870(1)° for the Ru and Os systems respectively. There was also no site mixing found between the Nd and Na atomic positions. Also, as expected for double perovskite systems with a charge difference of +4 between the B and B' sites,[29] the Rietveld refinements confirm that there is essentially no site mixing between the Na and B' atomic positions. It is

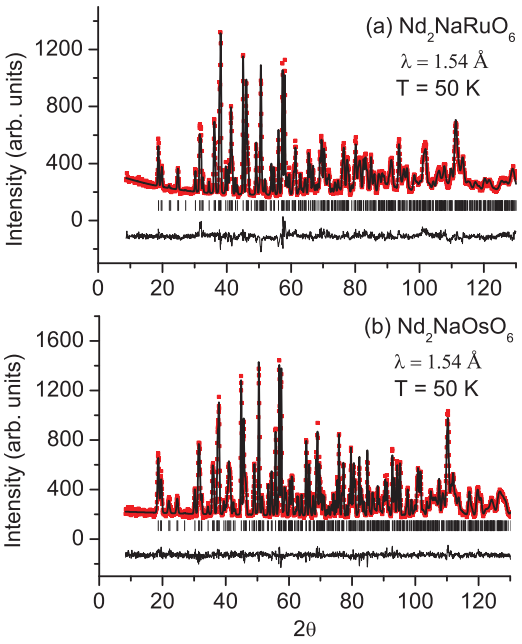

FIG. 2. (Color online) Neutron powder-diffraction measurements with a wavelength of 1.54 Å at $T = 50$ K for both (a) Nd_2NaRuO_6 and (b) Nd_2NaOsO_6.

worth noting that there are some double perovskites such as Ba_2YMoO_6, where B and B' site mixing is not observed in neutron diffraction, but picked up in magic-angle spinning NMR at the 1–3% level.[3]

As indicated by the $\lambda = 2.41$ Å NPD data presented in Fig. 3, at low temperatures additional scattering is observed in both the Nd_2NaRuO_6 and Nd_2NaOsO_6 neutron-diffraction patterns at commensurate positions. The magnetic scattering can be indexed on the basis of a propagation vector $\vec{k} = 0$ for the Ru system and $\vec{k} = (0.5\ 0.5\ 0)$ for the Os analog. Figure 3(c) shows the temperature dependence of the magnetic intensity for the Nd_2NaRuO_6 (0 1 0) magnetic reflection. A fit to the power law $I = A(T_c - T)^{2\beta}$ finds $T_c = 14.3(1)$ K and $\beta = 0.48(2)$. A similar plot of the (0.5 0.5 1) magnetic reflection intensity for Nd_2NaOsO_6 and subsequent power-law fit, shown in Fig. 3(f), indicates $T_c = 16.2(2)$ K and $\beta = 0.50(3)$. The critical exponents for the two systems both correspond to the value expected for mean-field theory. For the Os material, a series of powder-diffraction patterns were collected between 4 and 20 K to investigate the potential change in the magnetic structure suggested by previous susceptibility measurements around 10 K,[20] but no change in the magnetic structure was observed in this temperature range.

Representational analysis allowed the possible magnetic structures for these materials to be constrained on the basis of the crystal symmetry. The diffraction data were first modeled assuming magnetic ordering of only the Ru or Nd moments at the transition, but it quickly became clear that these assumptions could not explain the data. There are only two irreducible representations consistent with coupled Nd and Ru spin ordering and the observed propagation vector for Nd_2NaRuO_6; these are Γ_1 and Γ_3 in Kovalev's notation.[30] One of the main differences between these two magnetic structures is the spin components that are coupled ferromagnetically.

TABLE I. Structural parameters for Nd_2NaRuO_6 and Nd_2NaOsO_6 at $T = 4$ K extracted from the $\lambda = 1.54$ Å neutron powder-diffraction data.

(a) Nd_2NaRuO_6
Space group $P2_1/n$
$a = 5.4808(2)$ Å
$b = 5.9016(2)$ Å
$c = 7.8728(3)$ Å
$\beta = 90.898(3)^\circ$
$\chi^2 = 6.12$
$R_{wp} = 8.31\%$

Atom	Site	x	y	z
Nd	4*e*	0.4837(8)	0.0750(5)	0.2534(6)
Na	2*a*	0	0	0
Ru	2*b*	0.5	0.5	0
O_1	4*e*	0.209(1)	0.328(1)	0.0518(7)
O_2	4*e*	0.614(1)	0.4512(9)	0.2298(7)
O_3	4*e*	0.331(1)	0.781(1)	0.0660(7)

(b) Nd_2NaOsO_6
Space group $P2_1/n$
$a = 5.5128(1)$ Å
$b = 5.8932(1)$ Å
$c = 7.9242(1)$ Å
$\beta = 90.870(1)^\circ$
$\chi^2 = 1.14$
$R_{wp} = 5.50\%$

Atom	Site	x	y	z
Nd	4*e*	0.4818(4)	0.0698(3)	0.2533(3)
Na	2*a*	0	0	0
Os	2*b*	0.5	0.5	0
O_1	4*e*	0.2086(5)	0.3268(5)	0.0504(3)
O_2	4*e*	0.6155(5)	0.4498(4)	0.2307(3)
O_3	4*e*	0.3380(5)	0.7805(4)	0.0658(3)

More specifically, the spin components along the b axis are ferromagnetically coupled for both sublattices in the Γ_1 representation, while the spin components along both the a and c axes are ferromagnetically coupled in the Γ_3 representation. The neutron-diffraction data show no magnetic intensity at the (020) position, while there is significant magnetic intensity at the (200) and (002) positions. These observations are only consistent with the Γ_1 spin model, and this refinement is illustrated in Fig. 3(b) with the corresponding magnetic structure shown in Fig. 4(a). The Nd spins form a canted arrangement with a moment size of $2.31(3)\mu_B$ per Nd. The best refinement results in a type-I AF ground state for the Ru sublattice, with an ordered Ru moment of $1.62(8)\mu_B$. Since the Ru^{5+} magnetic form factor has not been accurately measured, the estimate for $\langle j_0 \rangle$ given in Ref. 31 was used for this refinement. The data were also refined using the Ru^{3+} and Ru^{4+} magnetic form factors from Ref. 32 and the Ru moment was found to be $1.72(8)\mu_B$ and $1.67(8)\mu_B$ in these two cases. These results indicate that the refined Ru ordered moment is relatively insensitive to the specific Ru magnetic form factor used in the analysis. The magnetic properties of the Ru sublattice are very similar to the magnetism reported for several other Ru^{5+} double perovskites,[33–37] and the coupled

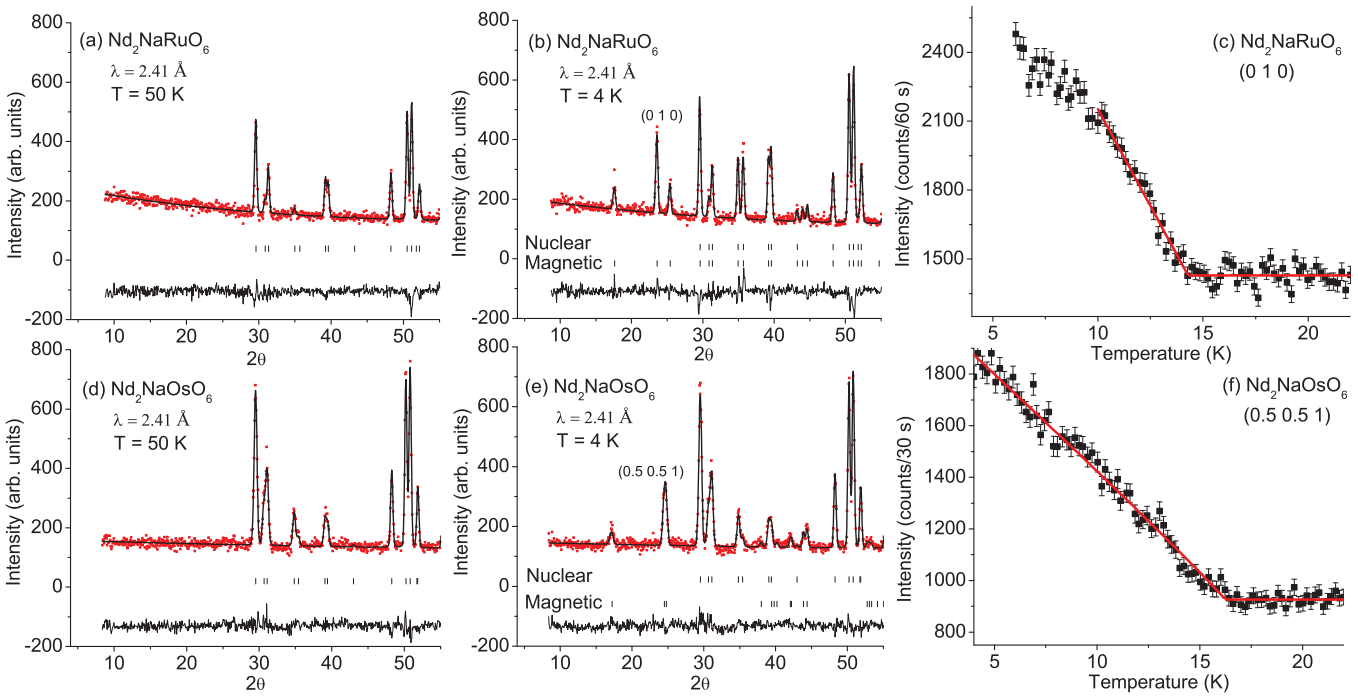

FIG. 3. (Color online) Neutron powder-diffraction data with $\lambda = 2.41$ Å is shown for Nd_2NaRuO_6 at (a) $T = 50$ K and (b) $T = 4$ K. The magnetic refinement at 4 K corresponds to the Γ_1 representation. (c) A plot of the magnetic intensity from HB-1A at the (0 1 0) position for Nd_2NaRuO_6, showing an increase in intensity below the magnetic transition at $T = 14.3(1)$ K. Neutron powder-diffraction data with $\lambda = 2.41$ Å is shown for Nd_2NaOsO_6 at (d) $T = 50$ K and (e) $T = 4$ K. The magnetic refinement at 4 K corresponds to the $\Gamma_2 - \Gamma_4$ model, as explained in the text. (f) A plot of the magnetic intensity from HB-1A at the (0.5 0.5 1) position for Nd_2NaOsO_6, showing an increase in intensity below the magnetic transition at $T = 16.2(2)$ K. The solid curves in (c) and (f) are power-law fits as described in the text.

Ru-Nd spin ordering is exactly what was observed in the related double perovskites R_2LiRuO_6.[23]

A similar situation was encountered for the Os sample, as no suitable magnetic models were found when assuming that only the Nd or Os spins ordered at the magnetic transition. There are also only two magnetic models allowed by symmetry that are consistent with coupled Nd and Os spin ordering and the observed propagation vector for Nd_2NaOsO_6. In Kovalev's notation,[30] these two models are superpositions of the Γ_2 and Γ_4 irreducible representations and can be described as $\Gamma_2 + \Gamma_4$ and $\Gamma_2 - \Gamma_4$. The basis vectors and the refined moments for these two models are indicated in Table II. A nonzero Os moment is critical to account for the full intensity of the magnetic peak at (0.5 0.5 0) in each case. The magnetic refinements were performed using the Os^{5+}

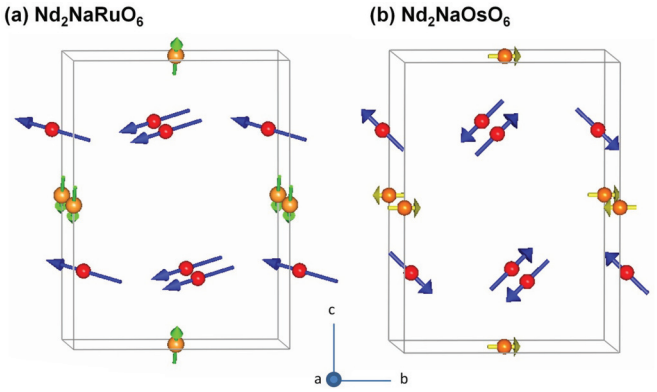

FIG. 4. (Color online) The magnetic structures determined from the neutron powder-diffraction data for (a) Nd_2NaRuO_6 and (b) Nd_2NaOsO_6 ($\Gamma_2 - \Gamma_4$ model). The B' sublattices exhibit type-I AF order, while the Nd spins form different canted arrangements. In each picture, the longer arrows (blue) represent the Nd moments and the shorter arrows (yellow/green) represent the B' moments.

TABLE II. Magnetic models and refined magnetic moments for Nd_2NaRuO_6 and Nd_2NaOsO_6.

	Ru Γ_1	Os $\Gamma_2 + \Gamma_4$	Os $\Gamma_2 - \Gamma_4$
B'_1	$[v_1, v_2, v_3]$	$[v_1, v_2, v_3]$	$[v_1, v_2, v_3]$
B'_2	$[-v_1, v_2, -v_3]$	$[-v_1, v_2, -v_3]$	$[v_1, -v_2, v_3]$
Nd_1	$[w_1, w_2, w_3]$	$[w_1, w_2, w_3]$	$[w_1, w_2, w_3]$
Nd_2	$[-w_1, w_2, -w_3]$	$[w_1, -w_2, w_3]$	$[-w_1, w_2, -w_3]$
Nd_3	$[w_1, w_2, w_3]$	$[w_1, w_2, w_3]$	$[w_1, w_2, w_3]$
Nd_4	$[-w_1, w_2, -w_3]$	$[w_1, -w_2, w_3]$	$[-w_1, w_2, -w_3]$
B'_1, μ_x	1.29(6)	0	0
μ_y	0	0	0.9(1)
μ_z	1.0(1)	−0.64(9)	0
μ	1.62(8)	0.64(9)	0.9(1)
Nd_1, μ_x	−1.05(4)	0.1(1)	0.2(2)
μ_y	−1.98(3)	1.20(6)	1.16(9)
μ_z	0.56(5)	−1.18(8)	−1.1(1)
μ	2.31(3)	1.69(7)	1.6(1)
R_{mag}(%)	10.8	18.1	16.8

magnetic form factor from Ref. 38. The $\Gamma_2 - \Gamma_4$ model gives the best refinement, with the result illustrated in Fig. 3(e) and a picture of the magnetic structure depicted in Fig. 4(b). In this model, the Nd and Os moments refine to $1.6(1)\mu_B$ and $0.9(1)\mu_B$ respectively, with the Os sublattice forming a type-I AF arrangement with the spins aligned along the b axis. Unlike Nd_2NaRuO_6, the stacking of the ferromagnetic planes associated with the type-I AF order is along the [110] direction. The Nd moment for the Os system is significantly reduced compared to Nd_2NaRuO_6, suggesting that the size of the ordered B' moment affects the magnitude of the rare-earth moment. Another possibility for the Nd moment reduction in the Os compound is that small changes in the structure between the Ru and Os materials could lead to a slightly different local environment around the Nd site. As a result, one can have different crystal-field splittings and ground-state eigenfunctions describing the Nd moments in the two cases.

The B' sublattices of Nd_2NaRuO_6 and Nd_2NaOsO_6 exhibit conventional type-I AF order for $S = 3/2$ B' double perovskites despite the large monoclinic structural distortions. This is in sharp contrast to the unconventional magnetism found in the highly distorted compounds La_2NaRuO_6 and La_2NaOsO_6,[26] characterized by incommensurate magnetism and a drastically reduced ordered moment respectively. The Nd compounds actually have even larger monoclinic structural distortions than their La counterparts, but the B' magnetic ground states are exactly what one expects for undistorted systems with dominant B'-O-O-B' AF exchange interactions. The addition of the rare-earth magnetic sublattice seems to destroy the delicate balance of competing exchange interactions giving rise to the unconventional magnetism in the La systems and instead stabilizes simple, commensurate AF on the B' sublattice. The rare-earth ions introduce Nd-O-B' interactions into the systems. Although these new couplings are expected to be weaker than B'-O-O-B' extended superexchange, and this is supported by the nearly identical magnetic transition temperatures between the $La_2NaB'O_6$ and $Nd_2NaB'O_6$ compounds, they are strong enough to act as a significant perturbation and alter the magnetic ground state of the B' sublattice. The resulting magnetic structures are very similar to the spin arrangements reported for R_2LiRuO_6.[23]

Both the ordered Ru and Os moments of Nd_2NaRuO_6 and Nd_2NaOsO_6 are significantly reduced compared to the expected spin only value of $3\mu_B$. Based on Hund's rules, the octahedrally coordinated B' atoms of these systems possess orbital singlet ground states, therefore spin-orbit coupling should have a negligible effect on reducing the ordered moment size. However, strong covalency effects are often associated with $4d$ and $5d$ magnetic systems and have been suggested to lead to smaller moments in these materials, particularly in iridates[39] and osmates.[40,41] In fact, the Os atoms of Nd_2NaOsO_6 and $NaOsO_3$ (Ref. 40) are found in nearly identical, slightly distorted oxygen octahedral cages so covalency effects should be very similar in the two systems. This is consistent with the comparable Os ordered moments of the two materials: $1.0(1)\mu_B$ for $NaOsO_3$ and $0.9(1)\mu_B$ for Nd_2NaOsO_6. Furthermore, the difference in the B' ordered moment size for Nd_2NaOsO_6 and Nd_2NaRuO_6 can also be explained by covalency effects, as these are expected to be enhanced in the osmate, relative to the ruthenate, due to the extended nature of the Os $5d$ orbitals.

In conclusion, we have investigated the magnetic properties of the double perovskites Nd_2NaRuO_6 and Nd_2NaOsO_6 with neutron powder diffraction. Despite the large monoclinic structural distortions of these materials, the B' sublattices exhibit conventional type-I AF order, as observed for several $S = 3/2$ B' magnetic double perovskites. The Nd and B' ions are also found to order at the same magnetic transition temperature. The magnetic Nd sublattice creates Nd-O-B' couplings, effectively destroying the delicate balance of extended superexchange interactions that lead to unconventional magnetism in the highly distorted double perovskites La_2NaRuO_6 and La_2NaOsO_6. These results indicate that A-site magnetic rare earths play an essential role in the determination of the magnetic ground state for the B' sublattice in double perovskite systems.

This research was supported by the U.S. Department of Energy, Office of Basic Energy Sciences. A.A.A., C.d.l.C., and S.E.N. were supported by the Scientific User Facilities Division. The neutron experiments were performed at the High Flux Isotope Reactor, which is sponsored by the Scientific User Facilities Division. D.E.B., J.Y., and H.z.L. would like to acknowledge financial support through the Heterogeneous Functional Materials for Energy Systems (HeteroFoaM) Energy Frontiers Research Center (EFRC), funded by the U.S. Department of Energy, Office of Basic Energy Sciences, under Award No. DE-SC0001061.

*Author to whom correspondence should be addressed: aczelaa@ornl.gov.

[1] K.-I. Kobayashi, T. Kimura, H. Sawada, K. Terakura, and Y. Tokura, Nature (London) **395**, 677 (1998).

[2] G. A. Prinz, Science **282**, 1660 (1998).

[3] T. Aharen, J. E. Greedan, C. A. Bridges, A. A. Aczel, J. Rodriguez, G. J. MacDougall, G. M. Luke, T. Imai, V. K. Michaelis, S. Kroeker, H. D. Zhou, C. R. Wiebe, and L. M. D. Cranswick, Phys. Rev. B **81**, 224409 (2010).

[4] J. P. Carlo, J. P. Clancy, T. Aharen, Z. Yamani, J. P. C. Ruff, J. J. Wagman, G. J. Van Gastel, H. M. L. Noad, G. E. Granroth, J. E. Greedan, H. A. Dabkowska, and B. D. Gaulin, Phys. Rev. B **84**, 100404(R) (2011).

[5] T. Aharen, J. E. Greedan, C. A. Bridges, A. A. Aczel, J. Rodriguez, G. J. MacDougall, G. M. Luke, V. K. Michaelis, S. Kroeker, C. R. Wiebe, H. D. Zhou, and L. M. D. Cranswick, Phys. Rev. B **81**, 064436 (2010).

[6] C. R. Wiebe, J. E. Greedan, P. P. Kyriakou, G. M. Luke, J. S. Gardner, A. Fukaya, I. M. Gat-Malureanu, P. L. Russo, A. T. Savici, and Y. J. Uemura, Phys. Rev. B **68**, 134410 (2003).

[7] C. R. Wiebe, J. E. Greedan, G. M. Luke, and J. S. Gardner, Phys. Rev. B **65**, 144413 (2002).

[8]K. E. Stitzer, M. D. Smith, and H.-C. zur Loye, Solid State Sci. **4**, 311 (2002).
[9]A. S. Erickson, S. Misra, G. J. Miller, R. R. Gupta, Z. Schlesinger, W. A. Harrison, J. M. Kim, and I. R. Fisher, Phys. Rev. Lett. **99**, 016404 (2007).
[10]G. Chen, R. Pereira, and L. Balents, Phys. Rev. B **82**, 174440 (2010).
[11]G. Chen and L. Balents, Phys. Rev. B **84**, 094420 (2011).
[12]D. Serrate, J. M. de Teresa, and M. R. Ibarra, J. Phys.: Condens. Matter **19**, 023201 (2007).
[13]P. Baettig and N. A. Spaldin, Appl. Phys. Lett. **86**, 012505 (2005).
[14]R. Nechache, C. Harnagea, A. Pignolet, F. Normandin, T. Veres, L.-P. Carignan, and D. Menard, Appl. Phys. Lett. **89**, 102902 (2006).
[15]F. Bai, L. Shi, H. Zhang, Z. Zhong, W. Wang, and D. He, J. Appl. Phys. **111**, 07C702 (2012).
[16]M. Azuma, K. Takata, T. Saito, S. Ishiwata, Y. Shimakawa, and M. Takano, J. Am. Chem. Soc. **127**, 8889 (2005).
[17]J. B. Goodenough, *Magnetism and the Chemical Bond* (John Wiley & Sons Inc., New York, 1963).
[18]D. E. Bugaris and H.-C. zur Loye, Angew. Chem. Int. Ed. **51**, 3780 (2012).
[19]W. R. Gemmill, M. D. Smith, and H.-C. zur Loye, J. Solid State Chem. **177**, 3560 (2004).
[20]W. R. Gemmill, M. D. Smith, R. Prozorov, and H.-C. zur Loye, Inorg. Chem. **44**, 2639 (2005).
[21]W. R. Gemmill, M. D. Smith, and H.-C. zur Loye, J. Solid State Chem. **179**, 1750 (2006).
[22]S. J. Mugavero III, A. H. Fox, M. D. Smith, and H.-C. zur Loye, J. Solid State Chem. **183**, 465 (2010).
[23]S. J. Makowski, J. A. Rodgers, P. F. Henry, J. P. Attfield, and J. W. G. Bos, Chem. Mater. **21**, 264 (2009).
[24]M. J. Davis, S. J. Mugavero III, K. I. Glab, M. D. Smith, and H.-C. zur Loye, Solid State Sci. **6**, 413 (2004).
[25]S. J. Mugavero III, M. D. Smith, and H.-C. zur Loye, J. Solid State Chem. **178**, 200 (2005).
[26]A. A. Aczel, D. E. Bugaris, L. Li, J.-Q. Yan, C. de la Cruz, H. C. zur Loye, and S. E. Nagler, Phys. Rev. B **87**, 014435 (2013).
[27]J. Rodriguez-Carvajal, Physica B **192**, 55 (1993).
[28]A. S. Wills, Physica B **276**, 680 (2000).
[29]M. T. Anderson, K. B. Greenwood, G. A. Taylor, and K. R. Poppelmeier, Prog. Solid State Chem. **22**, 197 (1993).
[30]O. V. Kovalev, *Representations of the Crystallographic Space Groups*, 2nd ed. (Gordon and Breach, Switzerland, 1993).
[31]N. G. Parkinson, P. D. Hatton, J. A. K. Howard, C. Ritter, F. Z. Chien, and M.-W. Wu, J. Mater. Chem. **13**, 1468 (2003).
[32]D. T. Cromer and J. T. Waber, *Scattering Factors Computed From Relativistic Dirac-Slater Wave Functions* (Los Alamos National Laboratory, 1964).
[33]P. D. Battle and C. W. Jones, J. Solid State Chem. **78**, 108 (1989).
[34]P. D. Battle, J. B. Goodenough, and R. Price, J. Solid State Chem. **46**, 234 (1983).
[35]P. D. Battle and W. J. Macklin, J. Solid State Chem. **52**, 138 (1984).
[36]Y. Izumiyama, Y. Doi, M. Wakeshima, Y. Hinatsu, K. Oikawa, Y. Shimojo, and Y. Morii, J. Mater. Chem. **10**, 23264 (2000).
[37]Y. Doi, Y. Hinatsu, K. Oikawa, Y. Shimojo, and Y. Morii, J. Mater. Chem. **10**, 797 (2000).
[38]K. Kobayashi, T. Nagao, and M. Ito, Acta Cryst. **A67**, 473 (2011).
[39]B. J. Kim, H. Jin, S. J. Moon, J. Y. Kim, B. G. Park, C. S. Leem, J. Yu, T. W. Noh, C. Kim, S. J. Oh, J. H. Park, V. Durairaj, G. Cao, and E. Rotenberg, Phys. Rev. Lett. **101**, 076402 (2008).
[40]S. Calder, V. O. Garlea, D. F. McMorrow, M. D. Lumsden, M. B. Stone, J. C. Lang, J.-W. Kim, J. A. Schlueter, Y. G. Shi, K. Yamaura, Y. S. Sun, Y. Tsujimoto, and A. D. Christianson, Phys. Rev. Lett. **108**, 257209 (2012).
[41]S. Calder, M. D. Lumsden, V. O. Garlea, J.-W. Kim, Y. G. Shi, H. L. Feng, K. Yamaura, and A. D. Christianson, Phys. Rev. B **86**, 054403 (2012).